Fuel 235 (2019) 1475–1491

Contents lists available at ScienceDirect

Fuel

journal homepage: www.elsevier.com/locate/fuel

Full Length Article

Characterization of pyrolysis products from slow pyrolysis of live and dead vegetation native to the southern United States☆

Elham Amini[a], Mohammad-Saeed Safdari[a], Jonathan T. DeYoung[a], David R. Weise[b], Thomas H. Fletcher[a,*]

[a] Department of Chemical Engineering, Brigham Young University, Provo, UT 84602, USA
[b] USDA Forest Service, PSW Research Station, Fire and Fuels Program, Riverside, CA 92507, USA

ARTICLE INFO

Keywords:
Slow pyrolysis
Live plant
Biomass
Tar
Char
Light gas

ABSTRACT

Prescribed (i.e., controlled) burning is a common practice used in many vegetation types in the world to accomplish a wide range of land management objectives including wildfire risk reduction, wildlife habitat improvement, forest regeneration, and land clearing. To properly apply controlled fire and reduce unwanted fire behavior, an improved understanding of fundamental processes related to combustion of live and dead vegetation is needed. Since the combustion process starts with pyrolysis, there is a need for more data and better models of pyrolysis of live and dead fuels. In this study, slow pyrolysis experiments were carried out in a pyrolyzer apparatus under nitrogen atmosphere in two groups of experiments. In the first group, the effects of temperature (400–800 °C), a slow heating rate (5–30 °C min^{-1}), and carrier gas flow rate (50–350 ml min^{-1}) on yields of tar and light gas obtained from pyrolysis of dead longleaf pine litter were investigated to find the optimum condition which results in the maximum tar yield. The results showed that the highest tar yield was obtained at a temperature of 500 °C, heating rate of 30 °C min^{-1}, and sweep gas flow rate of 100 ml min^{-1}. In the second group of experiments, 14 plant species (live and dead) native to forests in the southern United States, were heated in the pyrolyzer apparatus at the optimum condition. A gas chromatograph equipped with a mass spectrometer (GC–MS) and a gas chromatograph equipped with a thermal conductivity detector (GC-TCD) were used to study the speciation of tar and light gases, respectively. The results showed that the tar composition is dominated by oxygenated aromatic compounds consisting mainly of phenols. The light gas analysis showed that CO and CO_2 were the dominant light gas species for all plant samples on a dry wt% basis, followed by CH_4 and H_2.

1. Introduction

Wildland fire is an important ecological component of many ecosystems. Wildland fire can also damage or destroy life, property and natural resources. These hazards can be decreased with the proper application of prescribed burning which is the use of fire under specific fuel and weather conditions to obtain desired objectives such as hazardous fuel reduction, site preparation for seeding and planting, wildlife habitat management, control of insects, diseases, and weeds, and bio-diversity maintenance [1–3].

As solid fuels are heated, water in the surface layers evaporates, then pyrolysis occurs, followed by combustion of the volatiles and remaining solid (often called char). As part of a project measuring and modeling pyrolysis at different fuel scales, the focus of this component is the slow pyrolysis process of live and dead vegetation. Studying pyrolysis at low heating rates is needed for understanding the behavior of preheating and/or smoldering, as well as providing data to evaluate pyrolysis models over a wider range of heating rates. Knowledge gained from the larger project will hopefully improve our understanding of and ability to model wildland fire (open burning). Pyrolysis of biomass is also important for many other industrial applications involving biomass utilization. Pyrolysis is thermal decomposition of a material that occurs prior to combustion without requiring O_2 [4,5]. Depending on the environmental conditions, pyrolysis processes can be classified into three main categories: slow pyrolysis (slow heating rates, temperatures less than 500 °C residence time greater than 20 s), moderate pyrolysis

☆ This manuscript was prepared in part by a federal government employee as a part of his official duties and is therefore in the public domain and not subject to copyright.

* Corresponding author.
E-mail address: tom_fletcher@byu.edu (T.H. Fletcher).

https://doi.org/10.1016/j.fuel.2018.08.112
Received 28 June 2018; Received in revised form 17 August 2018; Accepted 24 August 2018
Available online 20 September 2018
0016-2361/

Table 1
List of plants used in slow pyrolysis experiments.

#	Common name	Scientific name	Type
1	Darrow's blueberry	Vaccinium darrowii	Broadleaf
2	Dwarf palmetto	Sabal minor	Palmetto
3	Fetterbush	Lyonia lucida	Broadleaf
4	Inkberry	Ilex glabra	Broadleaf
5	Live oak	Quercus virginiana	Broadleaf
6	Little bluestem	Schizachyrium scoparium	Grass
7	Longleaf pine foliage	Pinus palustris	Needle like
8	Longleaf pine litter	Pinus palustris	Needle like
9	Saw palmetto	Serenoa repens	Palmetto
10	Sparkleberry	Vaccinium arboreum	Broadleaf
11	Swamp bay	Persea palustris	Broadleaf
12	Water oak	Quercus nigra	Broadleaf
13	Wax myrtle	Morella cerifera	Broadleaf
14	Wiregrass	Aristida stricta	Grass
15	Yaupon	Ilex vomitoria	Broadleaf

(temperatures of 500 °C and residence time of 10–20 s), and fast pyrolysis (fast heating rates, temperatures greater than 500 °C, and residence time less than 2 s) [5].

Cellulose (~50% on dry basis), hemi-cellulose (20–40% in non-woody biomass and 10–30% in woody biomass) and lignin (10–40% in non-woody and 20–40% in woody biomass) are commonly identified as the three main components of biomass [6,7]. The ratio of these three components changes with the type of biomass, the part of the plant sampled, and other biomass characteristics [8]. These components mainly consist of alkanes, aromatics, esters, alcohols and ketones with different oxygen-containing structures [9]. Extractives, which are generally smaller organic molecules or polymers, are the other typical components in biomass [10,11]. Live fuels contain structural carbohydrates, non-structural carbohydrates, lipids, proteins, and sugars [12–14], which may impact combustion. Dead fuels have been found to have fewer extractives than live fuels; the amount varies among species [15].

There are two main steps for pyrolysis of solid fuel: primary and secondary pyrolysis. Primary pyrolysis occurs at relatively low temperatures, as the solid fuel decomposes to volatile gases and char. Primary pyrolysis produces light gases (such as CO, CO_2, H_2O, and H_2), tar, char, and mineral ash. The yields of these products depend on the heating rate, temperature, pyrolysis mode, solid residence time, reactor type, feed materials, and fuel properties [5,16]. There is a substantial body of research focused on studying the effects of these parameters [17–21] on biomass pyrolysis. Secondary pyrolysis is a process when the products of primary pyrolysis, especially tar, undergo further reactions at higher temperatures and longer residence times. Secondary pyrolysis reactions generally occur at temperatures above 500 °C for biomass tar [22,23]. Bio-char, or the residual solid, is generally high in carbon content and is the solid product of pyrolysis process. Tar is defined as the volatile species that will condense to solid or liquid when cooled to room temperature. Tar is a complex mixture consisting of a variety of organic components from different chemical groups such as aromatics, hydrocarbons, aliphatic compounds, and oxygenated compounds [24,25]. The organic compounds can be divided into low-polarity components (organic layer) and high-polarity components (water soluble) according to their water solubility. These components can be categorized as ketones, acids, phenols, aldehydes, ethers, hydrocarbons, esters, sugars, etc. [5,25–29]. The composition of tar predominately depends on the type of feedstock and can exceed 70 wt% on dry basis [5,30].

Heating rate and temperature are the main parameters that affect the decomposition of biomass. The lower pyrolysis temperatures and low heating rates favor the production of char. Higher pyrolysis temperatures, high heating rates, and long residence times lead to the formation of gas products. Studies have shown that the highest tar production yields are obtained at a reaction temperature around 500 °C, high heating rates, and with short vapor residence times for minimizing secondary reactions [24,30–35].

The fuel beds of wildland fires are heterogeneous in nature, contain different fuel components, and have a mixture of live and dead fuels [36]. These characteristics affect heat transfer, air flow, the combustion process and fire propagation. The burning behavior is different for live and dead fuels [37]. Fires that occur in the living crowns of woody shrubs and trees are often the most uncontrollable and unpredictable ones [38,39]. Living vegetation burns readily when moisture content decreases and large fires can occur when moisture content approaches seasonal minimums.

Pyrolysis of biomass, such as dead and dried vegetation, as well as wood, has been explored in detail [21,40–43], especially for power systems. However, there is a lack of research in the field of pyrolysis of live fuels to support wildland fire research. Many fire models assume the fuel bed as homogenous, with properties taken from wet dead fuels, in some instances with higher heat content, and do not consider properties of live vegetation. However, subsequent research has shown

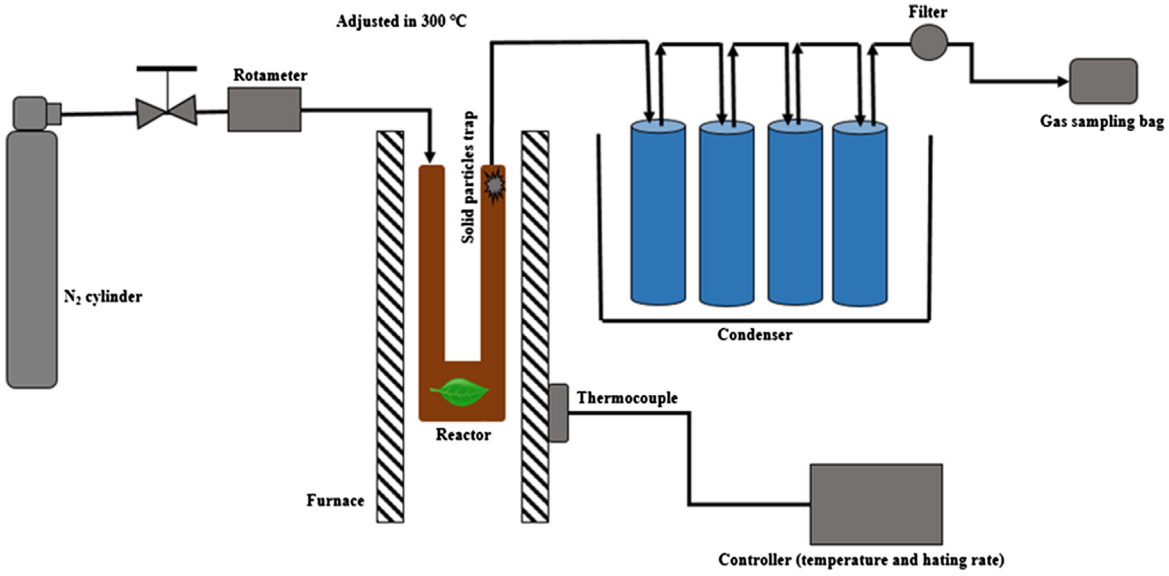

Fig. 1. Schematic of pyrolyzer apparatus used for slow pyrolysis.

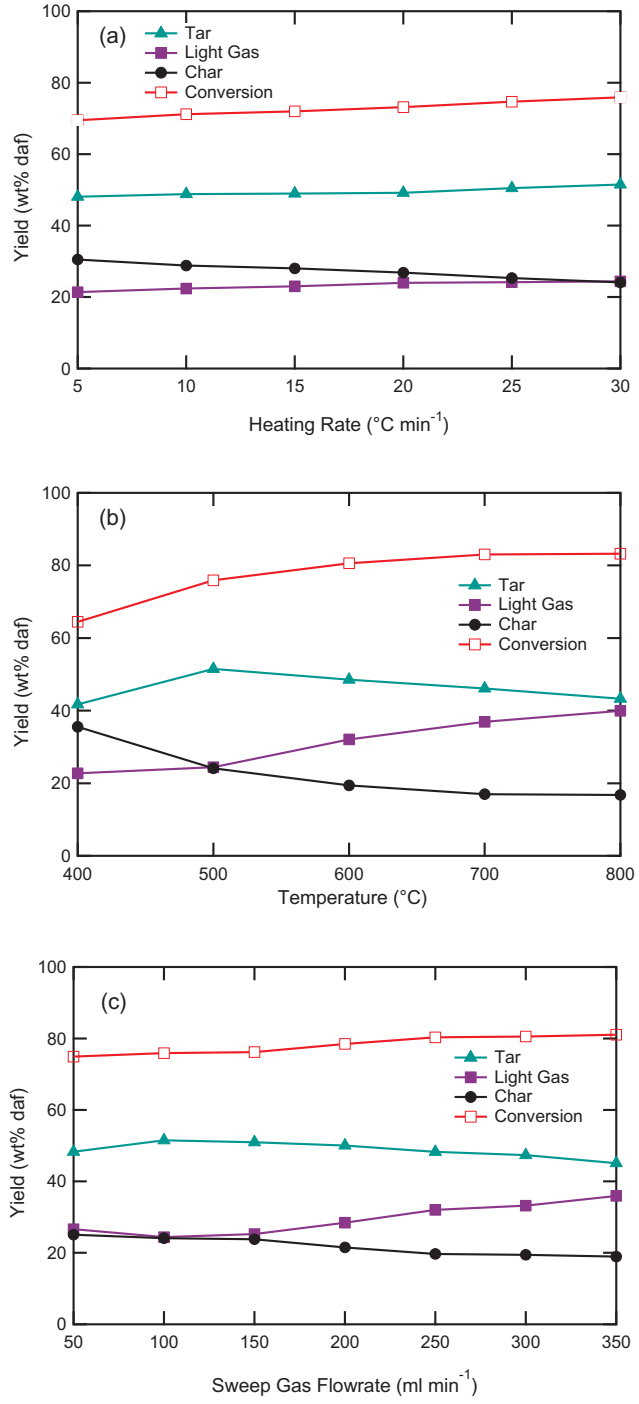

Fig. 2. Effect of pyrolysis: a) heating rate, b) temperature, and c) sweep gas flowrate on conversion and product yields (daf).

this assumption to be in error [44] and new models are being developed [45]. Live and dead fuels can be distinguished by the moisture content. Fuels with no metabolic activity are dead and typically have moisture contents (m_{H2O}/m_{dry}) less than 30–35% because of fiber saturation. Living plants (fuels) actively regulate water, while dead foliar fuels absorb/desorb water passively and typically may have an amount of moisture greater than 35% only if the water on the leaf surface is absorbed into the cell cavities [46]. This feature distinguishes wet dead fuel from live fuel [38].

The objective of this work is to provide fundamental information about slow pyrolysis products of live and dead plant species. The results of present work may help modelers develop a more accurate model of pyrolysis by presenting an improved understanding of the fundamental processes related to slow pyrolysis in heterogeneous fuel beds of live and dead fuels.

During this research, slow pyrolysis of 14 plant species (live and dead) native to forests in the southern United States, was studied using a pyrolyzer apparatus. These plant species were selected since they are commonly burned in prescribed fires. In related previous research, the characterization of pyrolysis products from fast pyrolysis (~100 K/s) of the same plant species were studied at a moderate temperature (765 °C) [44]. Tar and light gases analysis were studied using a gas chromatograph equipped with a mass spectrometer (GC–MS) and a gas chromatograph equipped with a thermal conductivity detector (GC-TCD), respectively.

2. Material and methods

2.1. Plant species

Table 1 lists the plant species used in pyrolysis experiments which were classified into 4 types: grasses, needle like, palmetto-type and broadleaf species. Photos of these species can be found elsewhere [44]. These plants were grown in a nursery and then express-mailed to the combustion laboratory at Brigham Young University (BYU) as live plants. These plants were kept alive with sufficient sunlight and regular watering. Plants are generally considered dead when the moisture content falls below 30% (m_{H2O}/m_{dry}). For the dead plant experiments in this work, plants were left for a minimum of one week to completely dry and reach a moisture content less than 10%.

It was not possible to conduct a study of aging for all dead samples. However, longleaf pine litter was studied, which is dead longleaf pine needles that have aged for several months and sold as bedding material. The pyrolysis products of live longleaf pine needles, freshly dried (and hence dead) longleaf pine needles, and longleaf pine litter were measured to study the effect of aging.

2.2. Proximate and ultimate analysis

The moisture content of plant samples was determined by placing a 5 gm sample in a Computrac MAX 1000[1] moisture analyzer. The ultimate and proximate analysis were measured by the University of Wisconsin Forage laboratory using ASTM D5291 and ASTM D7582 procedures, respectively, and reported by Safdari, et al. [44]. The elemental analysis provided in the ultimate analysis measured C, H, N, and S, but determined the O content by difference.

2.3. Pyrolysis setup

The pyrolyzer apparatus used in the present study is shown in Fig. 1. This pyrolyzer apparatus was previously used by Hillier et al. [47] to study the pyrolysis process of oil shale. The plant sample was placed intact into a metal tube and placed into an electrically-heated programmable furnace. The temperature of the furnace was controlled by a thermocouple connected to the controller. Gas condensers were constructed by packing fine glass wool into test tubes and using rubber stoppers to close the top. The gases entered and passed through the glass wool before exiting. The four condensers were placed in an ice bath filled with dry ice to aid condensation. The inlet tubing was connected to a nitrogen (carrier gas) cylinder. The outlet tubing from the heater was covered by heating tape (heated up to 300 °C) to avoid any possible condensation of organic vapors before entering the ice bath. A filter holder with filter paper was placed after the condensers to

[1] The use of trade or firm names in this publication is for reader information and does not imply endorsement by the U.S. Department of Agriculture of any product or service.

Table 2
Comparative studies for pyrolysis of different biomass to obtain maximum tar yield.

Biomass	Reactor	Temperature (°C)	Heating rate (°C min^{-1})	N_2 flow rate (ml min^{-1})	Wt% tar	Reference
Apricot pulps	Fixed-bed reactor	550	5	100	23.3[a]	Özbay et al. [62]
Pine needles	Semi-batch	550	50	100	43.8[b]	Varma and Mondal [61]
Ferula orientalis L.	Fixed-bed reactor	500	50	100	45.2[c]	Aysu and Küçük [60]
Blue-green algae blooms	Fixed-bed reactor	500	–	100	54.9[b]	Hu et al. [59]
Corncob	Fixed-bed reactor	500	40	100	26.4[a]	Demiral et al. [58]
Bamboo	Laboratory-scale pyrolysis reactor	500	10	70	36.5[b]	Chen et al. [57]
Jatropha curcas cake	Fixed-bed reactor	550	5	100	45.0[b]	Majhi et al. [63]
Tea waste	Fixed-bed reactor	500	300	200	29.6[b]	Uzun et al. [64]
Karanja seed	Semi batch reactor	550	–	50	55.1[b]	Shadangi and Mohanty [65]
Microalgae Scenedesmus dimorphus	Fixed-bed reactor	500	40	100	36.6[b]	Bordoloi et al. [66]
Hornbeam (Carpinus betulus L.) sawdust	Fixed-bed reactor	550	30	100	35.2[a]	Morali et al. [54]
Palm Shell	fluidized-bed reactor	500	–	2000 ml/min	47.3[b]	Abnisa et al. [67]

[a] Dry, ash-free basis.
[b] Basis is not mentioned in the literature.
[c] Ash-free basis, including water.

verify that tars did not travel downstream. The light gases coming out from the outlet of condensers were collected in a gas sampling bag for transfer to gas analysis devices. Before the pyrolysis experiment, nitrogen gas purged the reactor for 10 min to create an oxygen-free environment inside the reactor.

2.4. Experimental procedure

The pyrolysis experiments were conducted in the pyrolyzer apparatus by first weighing the u-shaped portion of the reactor. Second, a quantity of glass wool was fitted to the exit region of the reactor as a particle filter. For each pyrolysis experiment, approximately 2 g of sample were placed in the reactor. Whole leaves were folded (not cut) to fit into the reactor, with little or no stem material. Two groups of experiments were performed. In the first group, three sets of experiments were conducted with dead longleaf pine litter to find the optimum operating condition to obtain the highest tar yield. The first set of experiments was conducted with heating rates of 5, 10, 15, 20, 25, and 30 °C min^{-1} to a final temperature of 500 °C under constant flow rate of nitrogen at 100 ml min^{-1}, to investigate the effect of heating rate. The second set of experiments was conducted with a heating rate of 30 °C min^{-1} to final temperatures of 400, 500, 600, 700, and 800 °C, under nitrogen flow rate of 100 ml min^{-1}, to study the effect of temperature. The third set of experiments was conducted to determine the effect of sweep gas flowrate on product yields, with nitrogen flow rates of 50, 100, 200, 250, 300, and 350 ml min^{-1} to a final temperature of 500 °C with a heating rate of 30 °C min^{-1}. Three separate experiments were conducted at each heating rate, temperature, and sweep condition to determine repeatability.

The second group of experiments was performed at the optimum heating rate, temperature, and sweep gas flow rate for all 14 plant species (live and dead) to find the yields of light gas, tar, and char. Light gas and tar were subsequently analyzed for species composition. Three separate experiments were conducted for each species at this optimum condition to determine repeatability.

For each experiment, furnace temperature was held for a minimum of 1 h at the final temperature until no further release of gas was observed. The yield of char and liquid products were determined by weighing the reactor and the tar collection tubes before and after the experiment. The gas yield was calculated by difference.

2.5. Tar and gas analysis

Tar was removed from the glass wool and the sides of the test tubes using dichloromethane (DCM) as solvent. Water was removed from the tar/DCM solution by adding about 2 g anhydrous $CaSO_4$ powder. The decanted DCM/tar solution was analyzed off-line by an HP 5890 gas chromatograph (GC) equipped with an HP 5972 mass spectrometer (MS), and a Rxi®-1ms capillary column (60 m × 0.25 mm × 1.0 μm). Helium was used as a carrier gas with a constant flowrate of 2 ml min^{-1}. The temperature of the oven was held at 50 °C for 5 min, then increased to 310 °C with a rate of 10 °C min^{-1} and was held at this temperature for 5 min. 1 μL of sample with a split ratio of 10 was injected (1/10 of the sample goes through the column) [48]. The area under each peak represents the mole fraction of a component in the tar. These tar results must be viewed as semi-quantitative, since the system response for each tar molecule to relate moles to peak area was not determined, due to the large number (> 200) of peaks.

The light gas analysis was carried out in a ThermoFisher Scientific Trace 1310 gas chromatograph (GC) equipped with a thermal conductivity detector (TCD) and Chrompack Molsieve5A (25 m × 0.32 mm × 30 μm) and TracePLOT TG-Bond Q (30 m × 0.32 mm × 10 μm) columns [49,50]. Calibration standards for CO, CO_2, CH_4, and H_2 were used to make the light gas analysis quantitatively accurate. C_2H_6 and C_3H_8 were also run through the GC/TCD system to identify the retention times for the peaks for these species, but the peak heights for these species were so low in the pyrolysis experiments that detailed calibration was not performed.

2.6. Statistical analysis

All experiments were repeated three times. The statistical analysis was performed using the ANOVA data analysis tool in Microsoft Excel 2017 and the results are expressed as arithmetic mean values with a 95% confidence interval [51].

3. Results and discussion

3.1. Effect of pyrolysis temperature, heating rate, and sweep gas flowrate on product yields

The effect of pyrolysis temperature, heating rate, and sweep gas flowrate on product yields obtained from pyrolysis of dead longleaf pine litter was studied. The results are presented in Fig. 2. In the first set of experiments, the effect of heating rate on pyrolysis product yields at a temperature

of 500 °C was studied. From Fig. 2a, it can be seen that increasing the heating rate from 5 °C min^{-1} to 30 °C min^{-1} slightly increased the

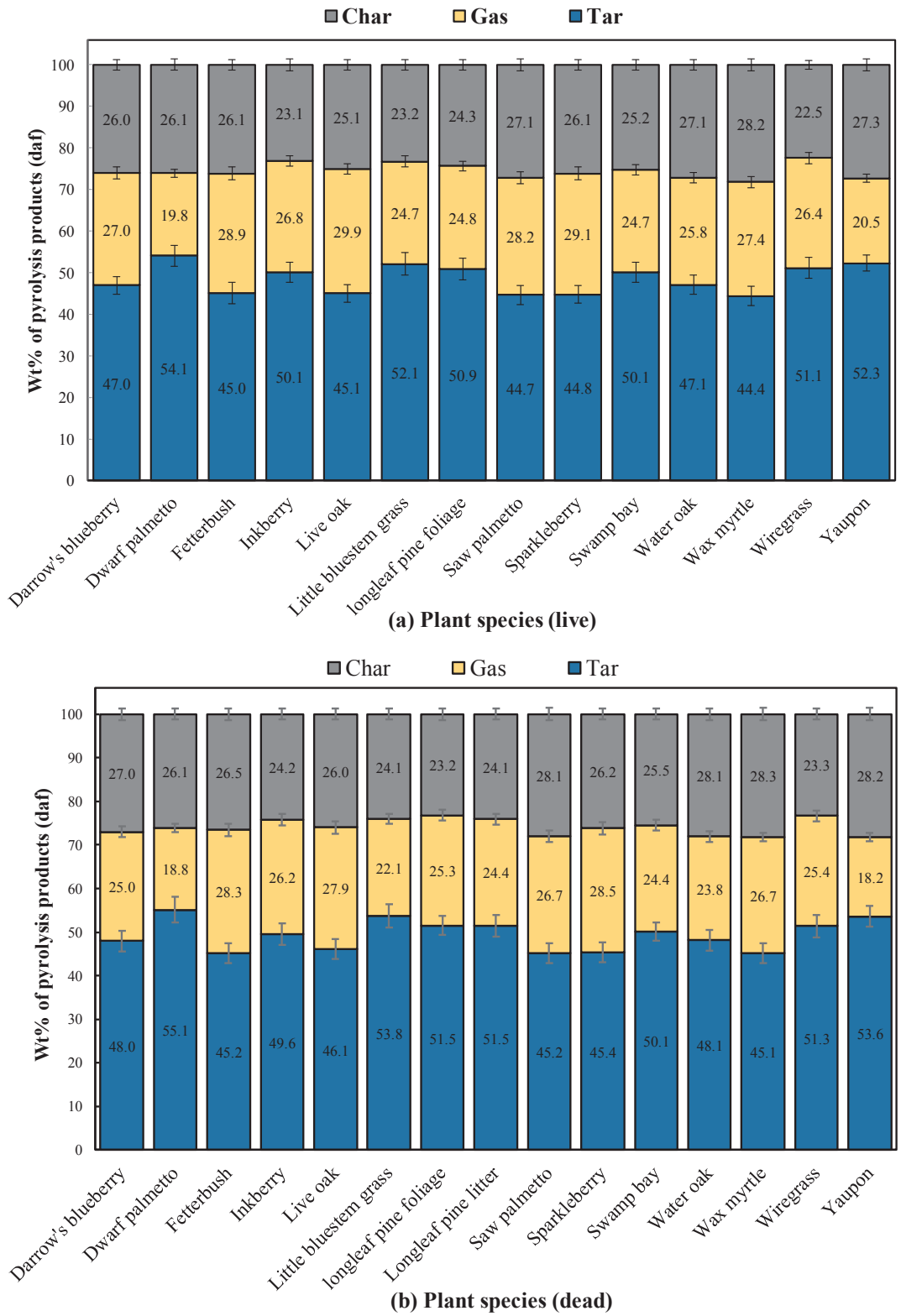

Fig. 3. Pyrolysis product distributions of (a) live and (b) dead plant species on a daf basis. Error bars represent the standard deviations based on three samples.

Table 3
Pyrolysis products variation for live and dead plant species.

Pyrolysis products (daf)	Live (wt%)	Dead (wt%)
Tar	44.4–54.1	45.1–55.1
Gas	19.8–29.1	18.8–30.4
Char	23.1–28.2	23.2–28.3

tar yield from 49.1 wt% to 51.5 wt% and decreased the char yield from 30.5 wt% to 24.1 wt%. The results of this study show that the change in heating rate had only a small effect on tar yield at these slow heating rates, but a greater impact on char yield.

In the second set of experiments, the effect of temperature on pyrolysis product yields was investigated. Fig. 2b shows the effect of temperature on biomass conversion and pyrolysis product yields on a

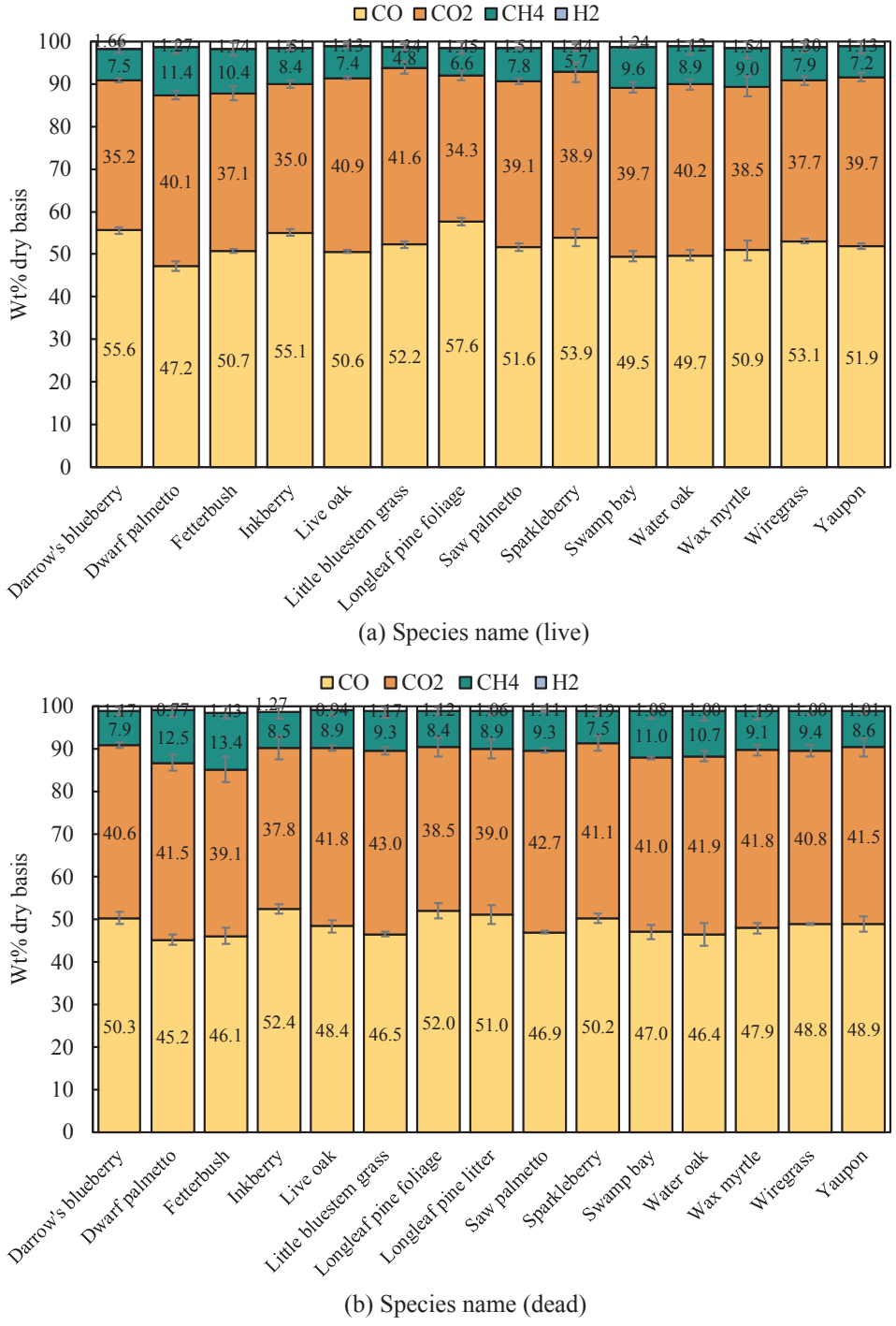

Fig. 4. Composition of light gases (dry basis) obtained from pyrolysis of: a) live and b) dead plants. Error bars represent the standard deviations based on three samples.

dry, ash-free (daf) basis. It can be seen that biomass conversion increases with increasing temperature due to extra energy inputs available to break the biomass bonds [52]. As temperature is increased from 400 to 500 °C, the tar yield increased from 41.7 wt% to 51.5 wt% at a heating rate of 30 °C min^{-1}. The highest tar yield was obtained at 500 °C for a heating rate of 30 °C min^{-1}. Beyond 500 °C, increasing the temperature negatively affected the tar yield. When temperature is increased from 500 °C to 800 °C, tar yields decreased from 51.5 wt% to 43.2 wt%. The most probable reason for a decreasing yield of tar at temperatures above 500 °C is the secondary cracking of volatiles at higher temperatures [25,53,54]. As seen from Fig. 2b, the char yield decreased from 35.5 wt% to 16.7 wt%, with increasing temperature at a heating rate of 30 °C min^{-1} from 400 °C to 800 °C that could be either due to greater primary decomposition of dead longleaf pine litter at higher temperatures or through secondary decomposition of char residue [55–57]. The increased temperature leads to an increased yield of gases from 22.7 wt% to 40.0 wt%. due to secondary cracking of pyrolysis vapors [55–57].

The third set of experiments was performed to study the effect of sweep gas flow rate on conversion and product yields by conducting the pyrolysis experiments with different nitrogen gas flow rates (50–350 ml min^{-1}) at a temperature and a heating rate of 500 °C and

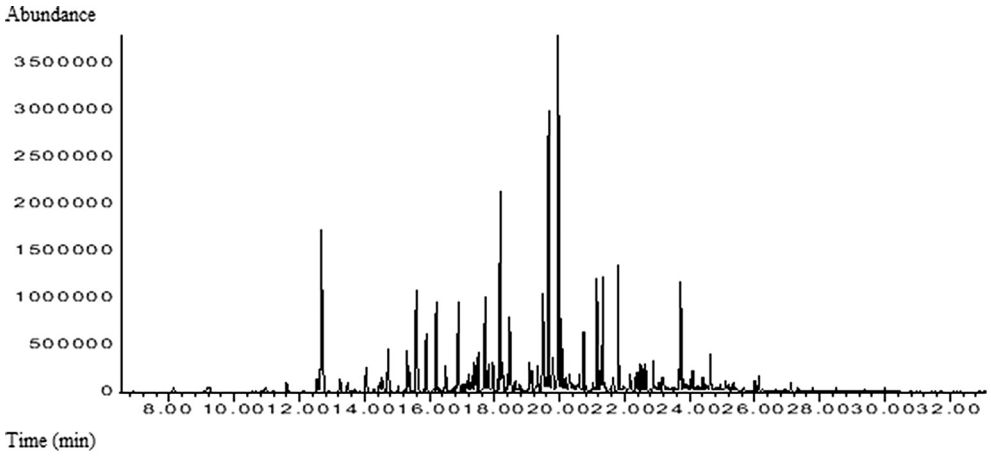

Fig. 5. GC–MS chromatograms of tar obtained at 500 °C for pyrolysis of longleaf pine litter.

30 °C min^{-1}, respectively. The maximum tar yield of 51.5 wt% was obtained at a flow rate of 100 ml min^{-1}. The conversion and tar yield were increased with increasing sweep gas flowrate from 50 to 100 ml min^{-1} and reached the maximum value at 100 ml min^{-1}. Beyond 100 ml min^{-1}, increasing the sweep gas flowrate decreased the tar yield. In contrast the char and gas yields, initially decreased with increasing the nitrogen gas flowrate from 50 to 100 ml min^{-1}, reaching the minimum values at 100 ml min^{-1}, and then increased with increasing the flowrate. The flowrate of sweep gas affects the residence time of the vapor phase obtained from pyrolysis. The role of sweep gas is to help the products to leave the hot zones quickly and minimize the secondary reactions such as thermal cracking, recondensation and repolymerization and maximize the yield of tar [58,59]. However, higher flow rates leads to decrease in liquid product yields and increase in gaseous product yields due to either inadequate cooling or fast exit of pyrolysis vapors from cooling zones [59,60].

In this study, it was found that pyrolysis temperature has the most important effect on product yields. A temperature of 500 °C, heating rate of 30 °C min^{-1}, and sweep gas flowrate of 100 ml min^{-1} was the optimum condition to produce the highest amount of tar from slow pyrolysis of dead longleaf pine litter. The standard deviation for these data was less than 5%, showing excellent data reproducibility. The range of tar yields obtained in this study (41.7–51.5 wt%) for longleaf pine litter are in the range of tar yields that have been reported in the literature (23.3–55.17 wt%) for different kinds of biomass in general [54,57–67], and specifically with the maximum tar yield of 43.8% reported by Varma and Mondal [61] for pine needles. Table 2 represents the optimum operation conditions for different biomasses reported in the literature for maximum tar yield.

3.2. Pyrolysis product distribution

Pyrolysis products distribution (tar, light gas, and char) depends on the several factors such as: plant species, reactor configuration, operating conditions, etc. The optimum pyrolysis operating condition with a temperature of 500 °C, heating rate of 30 °C min^{-1} and sweep gas flowrate of 100 ml min^{-1} found in the first series of the experiments was used to determine the pyrolysis products yields for all plant species (live and dead). Fig. 3 illustrates the product yields for live and dead plant species, respectively, obtained at the optimum tar yield condition. The results which are the average of three experiments are expressed on a dry, ash-free (daf) basis. The standard deviations for these data are shown as error bars in Fig. 3, showing excellent data reproducibility.

Table 3 shows the ranges of tar, gas, and char yields for live and dead plant species on a daf basis. Tar yields varied between 44.4 wt% and 54.1 wt% for live plants, and 45.1–55.1 wt% for dead plant species. The yields of light gas were in the range of 19.8–29.1 wt% for live plant species, and 18.8–30.4 wt% for dead plants. Char yields varied from 23.1 wt% to 28.2 wt% for live plant species, and between 23.2 and 28.3 wt% for dead plants.

The highest amount of tar was obtained from pyrolysis of dwarf palmetto (live and dead), with a yield of 54.1 wt% (daf). No significant differences were observed in pyrolysis product yields between live and dead plant samples for a specific plant species; the largest differences in tar yield (1.6 wt%) and char yield (1.1 wt%) were found between live and dead little blusteem grass and inkberry. Little bluestem grass showed the largest difference in gas yield (2.5 wt%) between live and dead plant samples. The dead plants exhibited slightly higher tar yields and slightly lower light gas yields in every case compared with the corresponding live plant samples, except for longleaf pine litter.

3.3. Light gas analysis

Fig. 4 represents the light gas compositions on a dry wt% (H_2O-free) basis resulting from slow pyrolysis of plant samples (live and dead) at the optimum operating condition of 500 °C with a heating rate of 30 °C min^{-1} and sweep gas flowrate of 100 ml min^{-1}. The standard deviations for these data are shown as error bars in Fig. 4, showing excellent data reproducibility. Despite slight differences due to type of plant, the gas composition for all plant species were similar and mainly consists of CO, CO_2, H_2, and CH_4. Gas species with higher carbon number (e.g., C_2H_6, C_3H_8, etc.) were not observed within the detection limits of ~1 mol%.

CO was the dominant compound in the light gases on a wt% dry basis, followed by CO_2, CH_4, and H_2 for both live and dead plant species. For live plant samples, CO yield ranged from 47.2 wt% for dwarf palmetto to 57.6 wt% for longleaf pine foliage. For dead plant samples, the yield of CO was between 45.2 wt% for dwarf palmetto and 52.4 wt% for inkberry. On average, the CO yield for live samples was 3.8 wt% (absolute) higher than the corresponding dead samples. The highest statistically difference in carbon monoxide composition between live and dead samples ($P < 0.05$) was observed in the little bluestem grass (5.7 wt% on an absolute basis), followed by longleaf pine foliage (5.6 wt%) and Darrow's blueberry (5.4 wt%).

CO_2 was the second most dominant light gas composition which varied between 34.4 wt% and 41.6 wt% for live plants, and 37.8 wt% and 43.0 wt% for dead plants. On average, the CO_2 yield for live samples was 2.5 wt% (absolute) lower than the corresponding dead samples. Darrow's blueberry demonstrated the largest statistically difference in carbon dioxide composition (5.4 wt%) between live and dead samples ($P < 0.05$). Longleaf pine foliage (4.2 wt%) and saw palmetto (3.6 wt%) had the next largest statistically differences ($P < 0.05$) in CO_2 composition between live and dead samples.

CH_4 yield varied from 4.8 wt% to 11.4 wt% for live plants and from

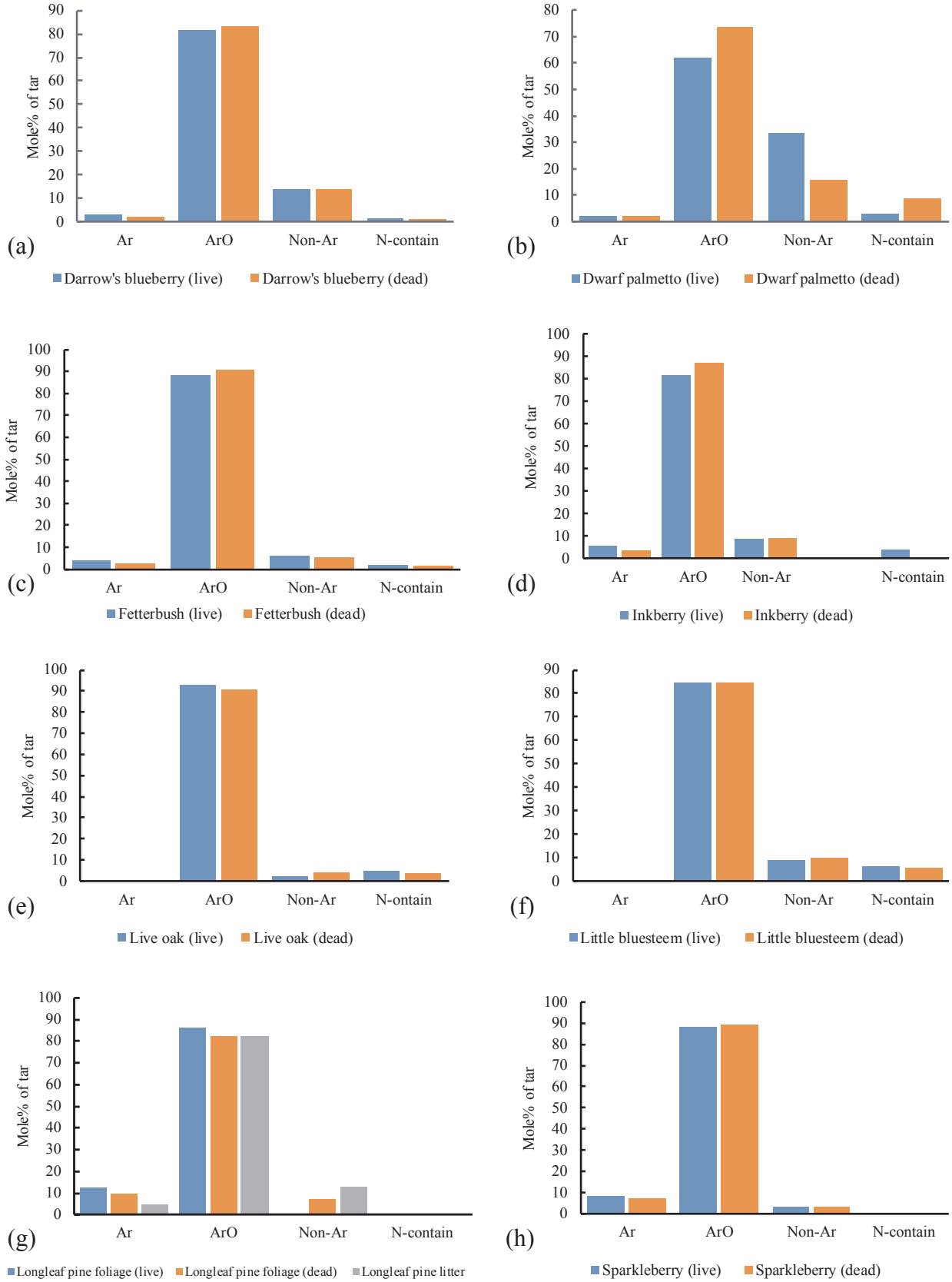

Fig. 6. The yields of tar components categorized as Ar, ArO, Non-Ar, and N-contain compounds for all plant species.

6.6 to 13.4 wt% for dead plants. On average, the CH_4 yield for live samples was 1.6 wt% (absolute) lower than the corresponding dead samples. The little bluestem grass showed the highest statistically difference in methane composition (4.5 wt%) between live and dead samples ($P < 0.05$).

The yield of hydrogen ranged between 1.12 and 1.74 wt% for live

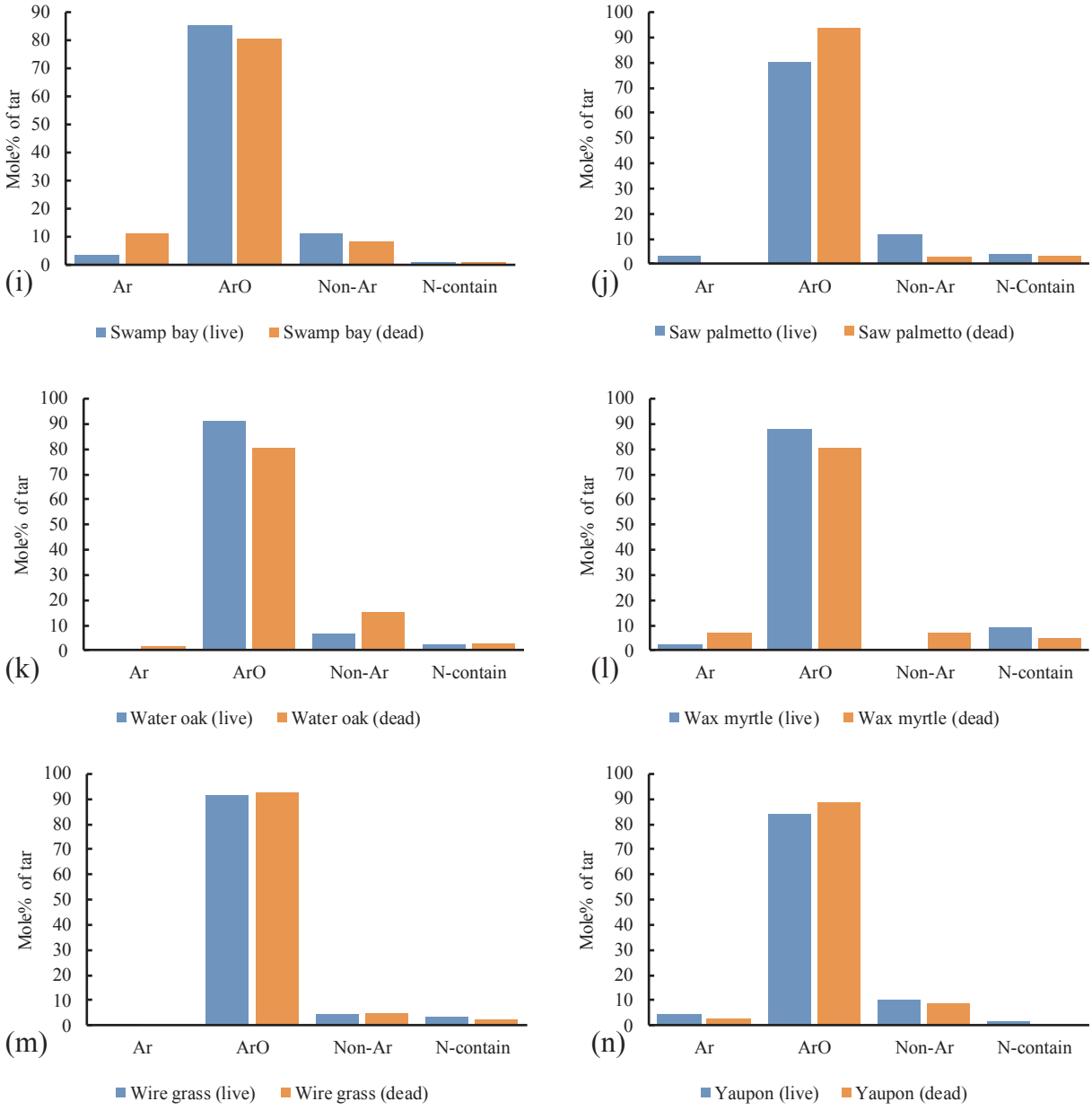

Fig. 6. (*continued*)

plants and between 0.77 and 1.19 wt% for dead plants. On average, the H_2 yield for live samples was 0.3 wt% (absolute) higher than the corresponding dead samples. The largest statistically differences ($P < 0.05$) between live and dead plant samples were observed in Dwarf palmetto (0.50 wt%), Darrow's blueberry (0.48 wt%), and saw palmetto (0.4 wt%).

The results of this study are supported by biomass pyrolysis literature where similar gas components were reported [61,68–70]. The main gas products from pyrolysis are formed from specific functional groups [9]. For example, the cracking and reforming of the carbonyl C═O, ether C—O—C, and carboxylic acid (COOH) are likely to produce CO, CO_2 at temperatures below 600 °C, and the formation of CH_4 is mainly due to the fracture of O—CH_3 groups [71]. The chemical structure of biomass components affects the chemical composition of the light gas products. For example, hemicellulose displays a higher CO_2 yield due to higher carboxyl content, and cellulose pyrolysis leads to a higher CO yield, mainly because of thermal cracking of carbonyl and carboxyl. The release of H_2 and CH_4 are mainly attributed to the pyrolysis of lignin [5,72].

3.4. Tar characterization

A typical GC–MS chromatogram of tar obtained from pyrolysis of longleaf pine litter at the optimum condition is given in Fig. 5. This is one example of more than 90 tar analysis experiments performed. Tars obtained from the slow pyrolysis of live and dead plant species in the pyrolyzer apparatus were a complex mixture of C_5-C_{20} organic aromatic (Ar), non-aromatic (Non-Ar), oxygenated aromatic (ArO), and some N-containing components (see Fig. 6).

More than 200 compounds were identified in tars obtained from slow pyrolysis of all plant species (live and dead); the most prevalent components are listed in Table 4. The distribution of these components in tar obtained from pyrolysis of all plant species are shown in Fig. 7. The standard deviations for these data are shown as error bars in Fig. 7, showing excellent data reproducibility. Phenolic compounds, such as phenol, 1,2-benzenediol, and phenol, 2-methyl which are belong to the ArO group are the most prevalent species in tar (Table 4). The other components belong to aldehyde, ketone, alcohol, furan, acid, and phenyl groups. Single-ring aromatics with OH attachments were the

Table 4
The most prevalent components observed in tar from these experiments.

#	Peak retention time (min)	Component	M.F.	Chemical class	Functional group	Structure
1	13.665	2(5H)-Furanone	$C_4H_4O_2$	ArO	Ketone	
2	12.681	Furfural	$C_5H_4O_2$	ArO	Aldehyde	
3	13.251	2-Furanmethanol	$C_5H_6O_2$	ArO	Alcohol	
4	14.72	2-Cyclopenten-1-one, 2-hydroxy-	$C_5H_6O_2$	ArO	Ketone	
5	15.893	Phenol	C_6H_6O	ArO	Phenol	
6	15.597	2-Furancarboxaldehyde, 5-methyl-	$C_6H_6O_2$	ArO	Aldehyde	
7	19.29	1,2-Benzenediol	$C_6H_6O_2$	ArO	Phenol	
8	20.599	1,3-Benzenediol	$C_6H_6O_2$	ArO	Phenol	
9	20.632	1,4-Benzenediol	$C_6H_6O_2$	ArO	Phenol	
10	14.147	Ethanone, 1-(2-furanyl)-	$C_6H_6O_2$	ArO	Ketone	
11	16.872	2-Cyclopenten-1-one, 2-hydroxy-3-methyl-	$C_6H_8O_2$	ArO	Ketone	
12	17.415	Propanoic acid, 2-propenyl ester	$C_6H_{10}O_2$	Non-Ar	Acid	
13	22.397	1,2,3-Benzenetriol	$C_6H_6O_3$	ArO	Phenol	
14	18.461	Maltol (Larixic acid)	$C_6H_6O_3$	ArO	Acid	
15	17.387	Phenol, 2-methyl-	C_7H_8O	ArO	Phenol	
16	16.971	Phenol, 3-methyl-	C_7H_8O	ArO	Phenol	
17	17.3	Phenol, 4-methyl-	C_7H_8O	ArO	Phenol	
18	16.779	2-Cyclopenten-1-one, 2,3-dimethyl-	$C_7H_{10}O$	ArO	Ketone	
19	17.739	Phenol, 2-methoxy-	$C_7H_8O_2$	ArO	Phenol	
20	20.312	1,2-Benzenediol, 3-methyl-	$C_7H_8O_2$	ArO	Phenol	
21	20.721	1,2-Benzenediol, 4-methyl-	$C_7H_8O_2$	ArO	Phenol	
22	20.579	1,2-Benzenediol, 3-methoxy-	$C_7H_8O_3$	ArO	Phenol	
23	21.001	Indole	C_8H_7N	N-Contain	Benzenoid	
24	19.666	Benzofuran, 2,3-dihydro-	C_8H_8O	ArO (2r)	Furans	
25	18.909	Phenol, 4-ethyl-	$C_8H_{10}O$	ArO	Phenol	
26	19.949	2-Methoxy-5-methylphenol	$C_8H_{10}O_2$	ArO	Phenol	
27	19.534	Phenol, 2-methoxy-4-methyl-	$C_8H_{10}O_2$	ArO	Phenol	
28	19.515	1,3-Benzenediol, 4-ethyl-	$C_8H_{10}O_2$	ArO	Phenol	
29	22.551	1,2-Benzenediol, 4-ethyl-	$C_8H_{10}O_2$	ArO	Phenol	
30	19.251	1,3-Benzodioxole, 2-methoxy-	$C_8H_8O_3$	ArO	Phenyl	
31	21.727	Phenol, 2,6-dimethoxy-	$C_8H_{10}O_3$	ArO	Phenol	
32	20.894	Phenol, 4-ethyl-2-methoxy-	$C_9H_{12}O_2$	ArO,	Phenol	
33	21.387	2-Methoxy-4-vinylphenol	$C_9H_{10}O_2$	ArO	Alcohol	
34	23.284	Phenol, 2-methoxy-4-(1-propenyl)-	$C_{10}H_{12}O_2$	ArO	Phenol	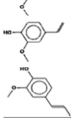

most dominant components observed in the tar obtained from live and dead samples at these conditions. Very few multi-ring components were observed. Due to the moderate temperature (500 °C) and the fact this temperature corresponded to the maximum tar yield, the tar species observed seem to be primary pyrolysis products, without being influenced by further "secondary" pyrolysis reactions in the gas phase.

Tar analysis results revealed that tar composition was different for different plant species. For example, phenol ranged from 1.9 mol% in dead longleaf pine litter to 38.69 mol% in dead dwarf palmetto. Dead saw palmetto and dead dwarf palmetto, which are from the same family, had very high phenol yields of 33.67 mol% and 38.69 mol%, respectively. A considerable difference in phenol composition in tar was observed for dead longleaf pine foliage and dead longleaf pine litter. While dead longleaf pine foliage had a phenol composition of 18.82 mol %, tar obtained from pyrolysis of longleaf pine litter contained only 1.9 mol% phenol. The results showed that the pyrolysis of dead longleaf pine foliage and dead longleaf pine litter yield different tar compositions at these experimental conditions and that metabolic process associated with foliage dehiscence or weathering once the needles have been cast are likely causes for the difference.

There are quite a few minor tar species with mole fractions less than 5 mol%. Some of these minor species (and occasionally major species)

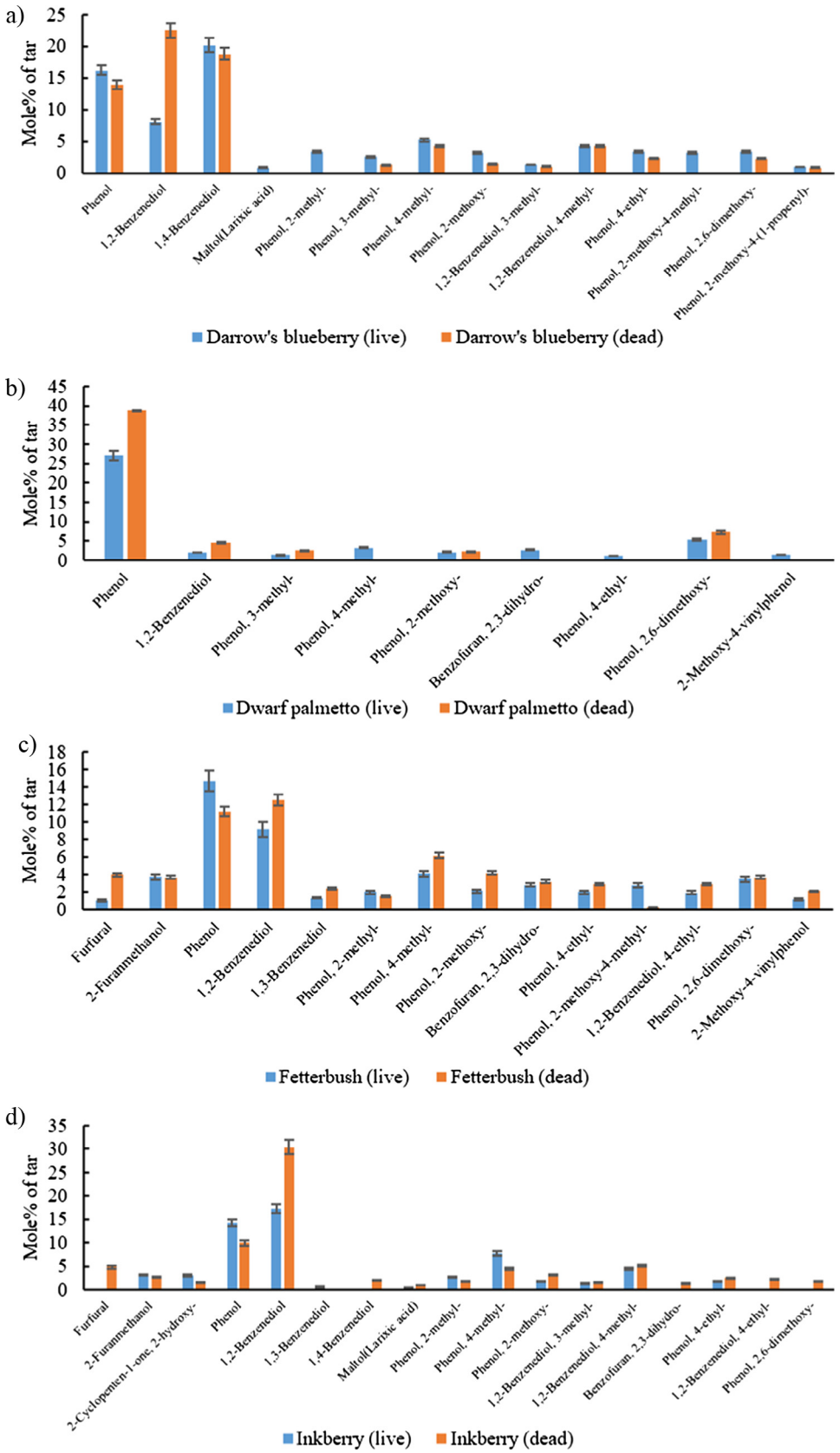

Fig. 7. The distribution of most prevalent components in tar obtained from pyrolysis of plant species. Error bars represent the standard deviations based on three samples.

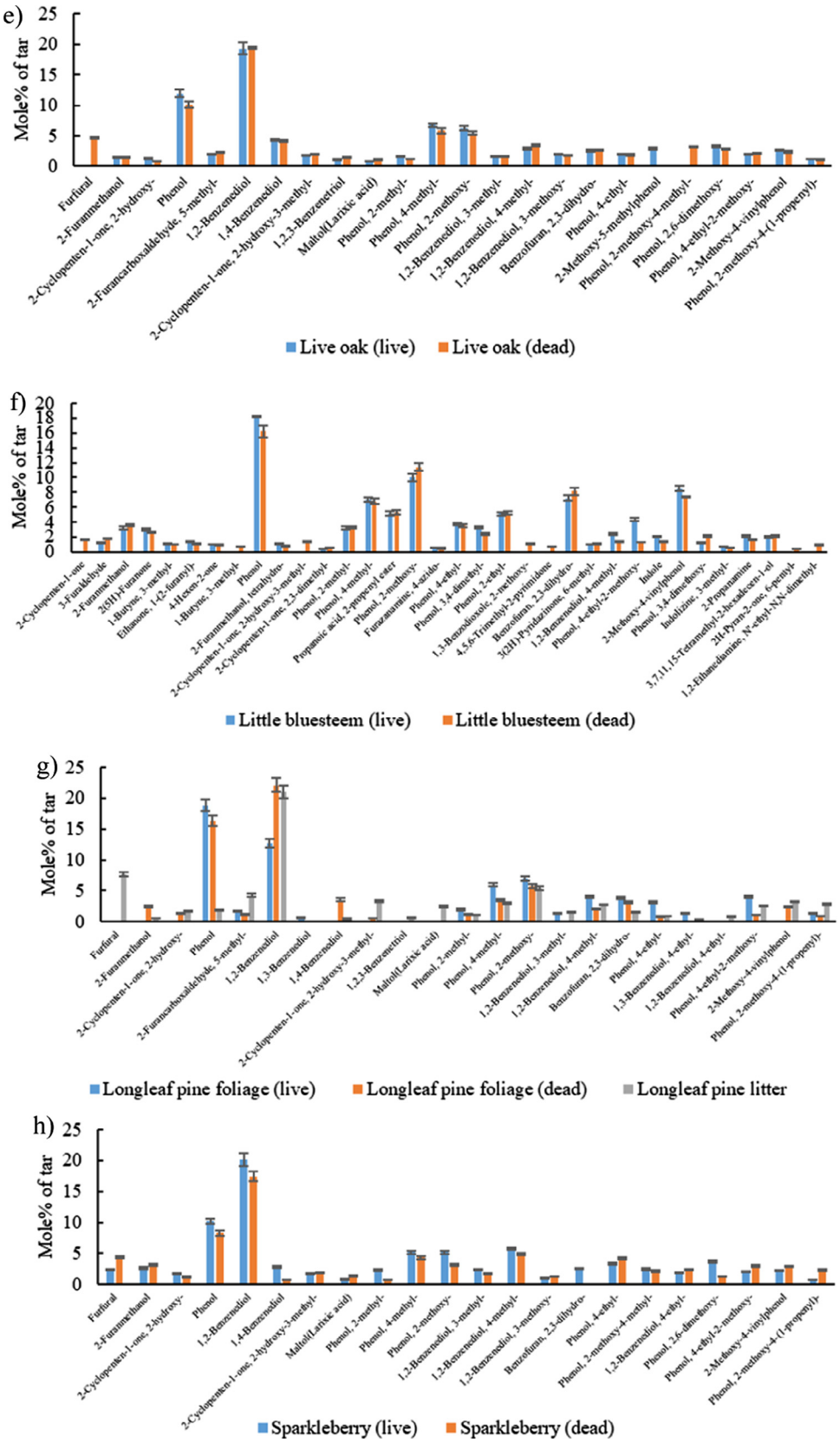

Fig. 7. (*continued*)

are only observed in the pyrolysis products from live samples, while others are only observed from dead samples. For example, tars from live water oak consisted of furfural (8 mol%), maltol (larixic acid) (1.5 mol %), 2-methyl phenol (1.4 mol%), 2-methoxy 5-methyl phenol (2.8 mol %), and 4 ethyl-1,3- benzenediol (0.8 mol%), none of which were observed in the tars from the dead water oak. However, 1,2,3 benzenetriol (1.1 mol%) and 2,3 dihydrobenzofuran (3.1 mol%) were only observed in the tars from dead water oak. Similar minor changes in tar species

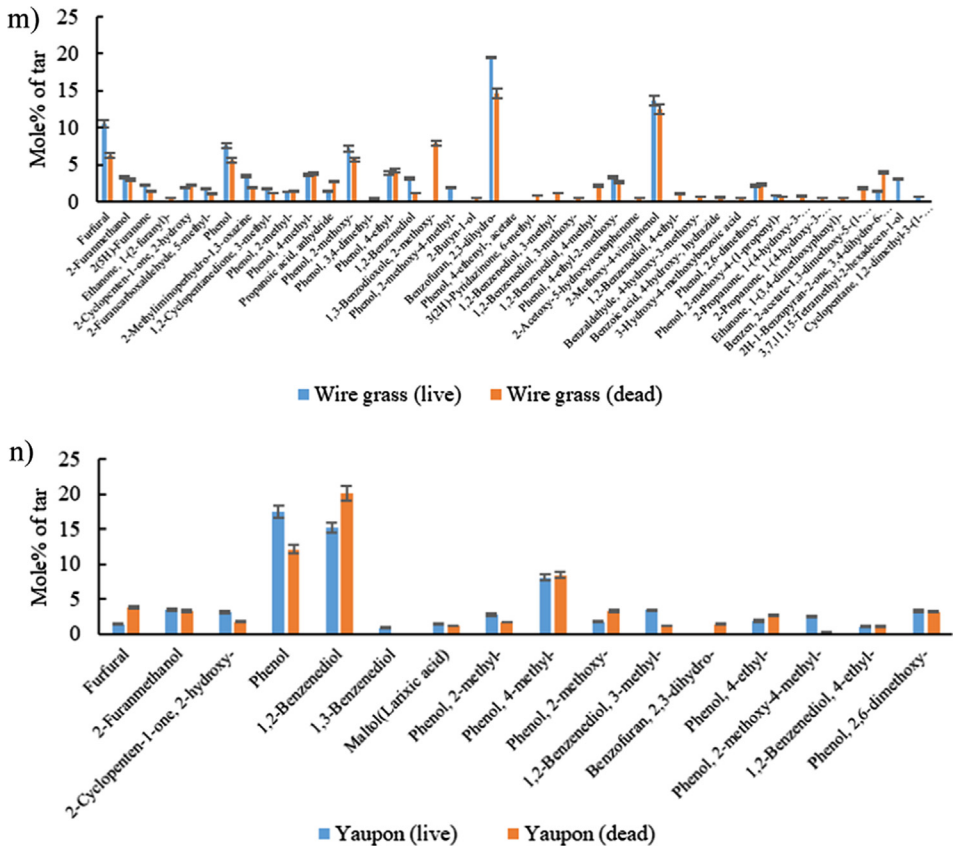

Fig. 7. (*continued*)

between live and dead samples were observed for other plant species. It is not clear how these relatively minor changes in tar species between live and dead plant species will change the combustion characteristics.

It has been reported that many of the components in tar are primary products of lignin degradation (280–500 °C) during pyrolysis [60]. The presence of phenolic hydroxyl and methoxyl groups in chemical structure of lignin makes it highly reactive. In general, phenols are mainly produced from the degradation of lignin which is a rich source of phenolic components; furans, ketones and carboxylic acids are thought to come from cellulose and hemicellulose degradation [60,69,71]. In addition, decomposition of lignin leads to the formation of aromatic carbons, since lignin contains aromatic rings in its chemical structure [73].

Hemicellulose has random amorphous structure with little strength which makes it highly activated in thermal decomposition. Generally, pyrolysis of hemicellulose (200–280 °C) mainly produces acids and furfural [60,71]. In contrast, cellulose has a good ordered structure with long polymer of glucose which make it thermally stable. Cellulose pyrolysis leads to a high tar yield [71], but not necessarily aromatic compounds. Furans, cyclopentanone, and linear carbonyls are mainly formed by depolymerization and fragmentation of active cellulose (240–350 °C) [71].

As shown in Fig. 6, ArO compounds were the most prevalent species in tar obtained from pyrolysis of all live and dead plant samples. The majority of aromatic compounds were one ring aromatics with OH attachments. As expected, plants from the same family have similar behavior in the formation of tar compounds. For example, the slow pyrolysis of dead saw palmetto and dead dwarf palmetto formed more ArO compounds than live samples. In contrast, tar obtained from slow pyrolysis of dead water oak and dead live oak contained less ArO compounds than live samples.

The volatiles yields obtained in this study are compared with the ASTM proximate analysis (reported by Safdari, et al. [44]) in Fig. 8. It can be seen that for most plant species the total volatiles yield from the ASTM analysis is a few absolute percentage points higher than the yields from the pyrolyzer apparatus due to the higher temperature (750 °C) of the ASTM analysis method. However, the 500 °C condition used in the pyrolyzer apparatus minimized secondary reactions of tar species, which was the aim of the present experiments.

3.4.1. Functional groups distribution in tar

Fig. 9 shows the functional groups distribution in tar obtained from slow pyrolysis of four plant species which are representative of palmetto-type, grass, broadleaf, and needle like species. Phenols which are the most prevalent components in tar obtained from pyrolysis of all plant types, ranged from 56.98 wt% for live dwarf palmetto to 70.47 wt % for live longleaf pine. Ketones, aldehydes, and acids which comprised a significant amount of the tars from all plant species, ranged between 4.73–19.20 wt%, 1.24–8.70 wt%, and 5.16–12.02 wt%, respectively. Moreover, furans comprised 4.34 wt% and 8.11 wt% of live longleaf pine (needle like species) and dead little bluestem (grass).

Differences between the distribution of functional groups in tar for live and dead plant samples were small. For example, tar obtained from the pyrolysis of live and dead longleaf pine contained 70.5 and 68.2 mol % phenols, respectively. Aldehydes comprised 6.0 mol% of the tar obtained from pyrolysis of live longleaf pine foliage vs. about 2.7 mol% from dead longleaf pine foliage.

In contrast, large differences were observed in the functional groups distribution in tars obtained from pyrolysis of different plant species. For live longleaf pine (needle like species), the tar contained more than 70 mol% phenolic compounds vs. 58.2 mol% phenolic compounds in tar from live Inkberry (broadleaf species).

4. Conclusion

Slow pyrolysis of 14 live and dead plant species native to the

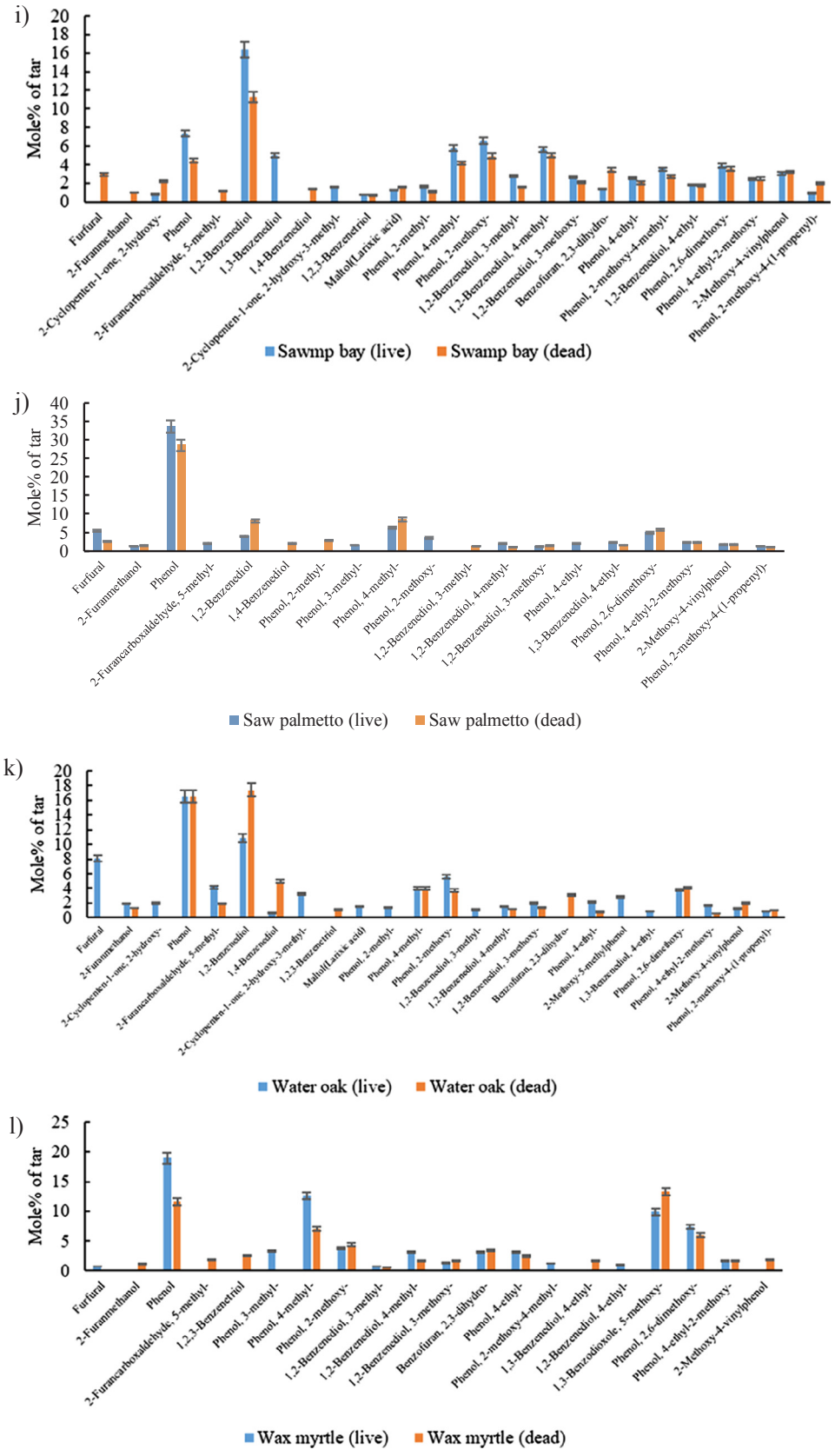

Fig. 7. (*continued*)

southern United states forests were studied using a pyrolyzer apparatus. Pyrolysis product distribution for all plant species were found and tar and light gas analysis were performed using GC–MS and GC-TCD, respectively. The most important results from this study are listed as follow:

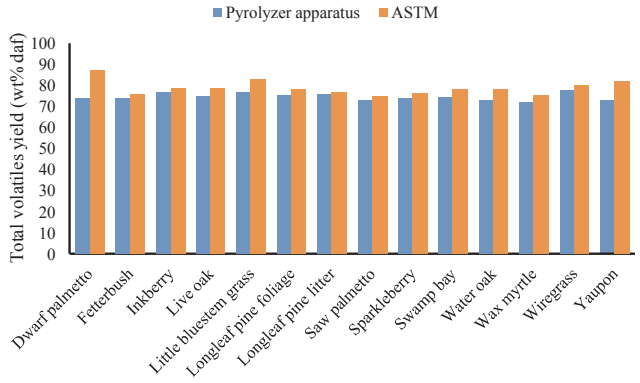

Fig. 8. Total volatiles yields obtained from slow pyrolysis experiments in pyrolyzer apparatus and ASTM analysis.

1- A pyrolysis operating condition with a temperature of 500 °C, heating rate of 30 °C min^{-1} and sweep gas flowrate of 100 ml min^{-1} was found as an optimum condition which yields the highest amount of tar from slow pyrolysis of dead longleaf pine litter.
2- Tar and gas species are the primary pyrolysis products, without being influenced by further secondary pyrolysis reactions in gas phase due to moderate temperature (500 °C).
3- Tar and light gas yields ranged between 44.4 and 54.1 wt% (daf) and 23.1–28.2 wt% (daf) for live plant samples, respectively.
4- Tar and light gas yields from live and dead plant samples of the same species differed only slightly.
5- Not only for tar species formed but also for pyrolysis product distribution and light gas analysis, the plant species appears to be more important than live vs dead samples.
6- CO was the dominant light gas species for all plant samples on a dry, wt% basis, followed by CO_2, CH_4 and H_2. Live plant species had slightly higher weight fractions of CO and H_2 (average differences of 3.8 and 0.3 wt% absolute, respectively) than corresponding dead samples, but slightly lower weight fractions of CO_2 and CH_4 (average differences of 2.5 and 1.6 wt% absolute, respectively).
7- The main constituents identified in the tar obtained from the slow pyrolysis of live and dead plant samples were oxygenated aromatics (ArO), which were mainly phenolic compounds (–OH).
8- Single-ring aromatics with OH attachments were the most prevalent compounds observed in the tar obtained from live and dead samples at these conditions. Very few multi-ring compounds were observed.
9- No significant differences between the distribution of functional groups in tar were observed for live and dead plant samples for a given plant species. In contrast, there were significant differences in the functional groups distribution in tars obtained from pyrolysis of different plant species.
10- Based on the product distributions observed in these experiments, differences in the fire behavior of live and dead fuels should be largely due to moisture content, since only small differences were observed in pyrolysis product distributions and tar components.

The results of this study can be used to investigate reactions that occur during slow pyrolysis and subsequent combustion of both live and dead plants. In addition, these data can help to find the heat release through slow pyrolysis of live and dead vegetation. Furthermore, these results can help modelers come up with more accurate models to predict prescribed burning behavior and fire propagation.

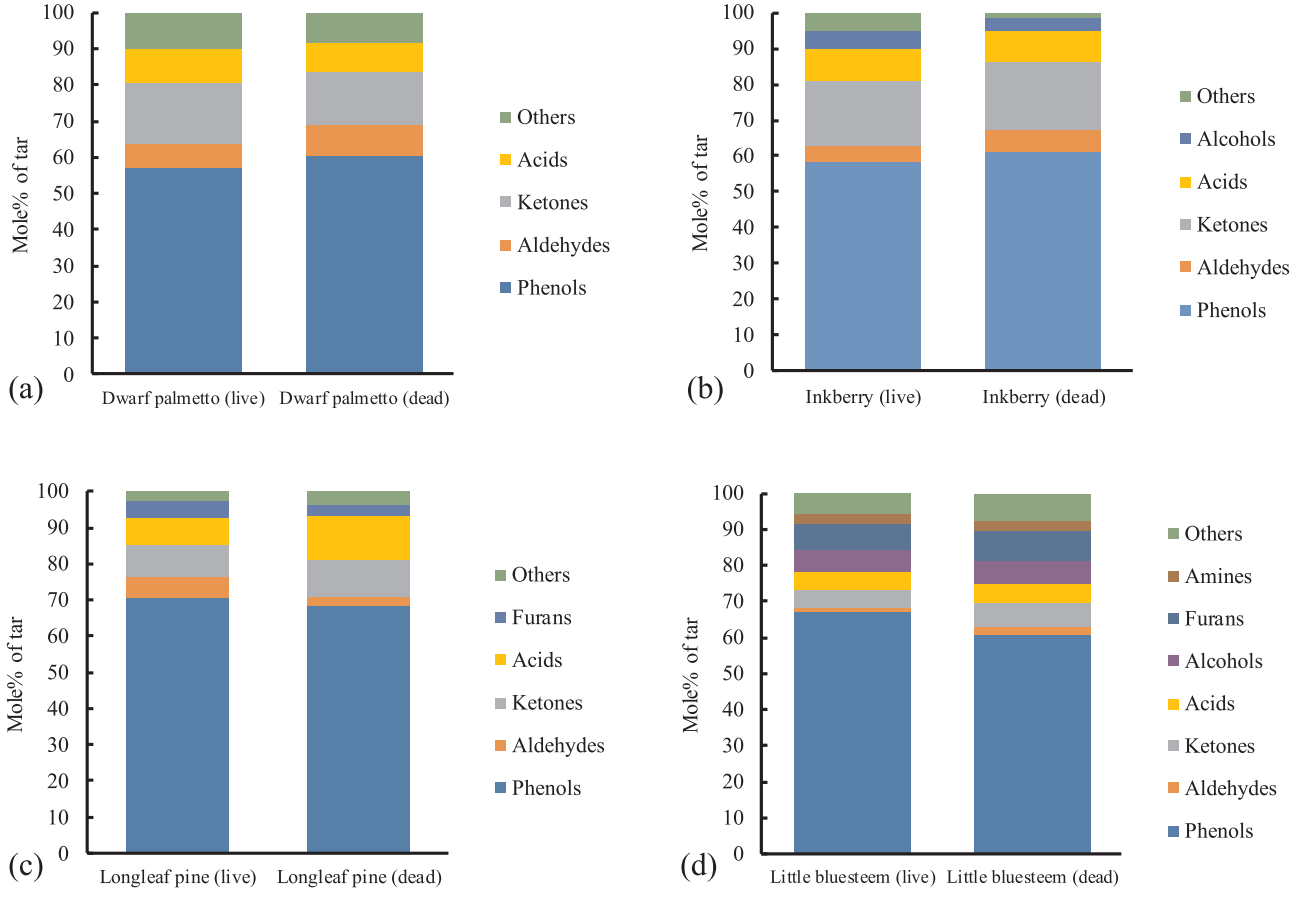

Fig. 9. Functional groups distribution in tar for live and dead plants.

Acknowledgements

This research was funded by DOD/EPA/DOE Strategic Environmental Research and Development Program Project RC-2640, funded thorough contrast 16-JV-11272167-024, administered by the USDA Forest Service PSW Research Station. Mark Dietenberger and Fred Matt of the USDA Forest Service Forest Products Lab provided the proximate and ultimate analyses of the plant species.

References

[1] Fernandes PM, Botelho SH. A review of prescribed burning effectiveness in fire hazard reduction. Int J Wildland Fire 2003;12:117–28.
[2] Wade DD, Lunsford JD. A guide for prescribed fire in southern forests, USDA Forest Service Technical Publication R8-T5 11. Atlanta, GA; 1989.
[3] Ferguson SC, Dahale A, Shotorban B, Mahalingam S, Weise DR. The role of moisture on combustion of pyrolysis gases in wildland fires. Combust Sci Technol 2013;185:435–53.
[4] Antonakou E, Lappas A, Nilsen MH, Bouzga A, Stocker M. Evaluation of various types of al-mcm-41 materials as catalysts in biomass pyrolysis for the production of bio-fuels and chemicals. Fuel 2006;85:2202–12.
[5] Dhyani V, Bhaskar T. A comprehensive review on the pyrolysis of lignocellulosic biomass. Renew Energy 2017.
[6] Haykiri-Acma H, Yaman S, Kucukbayrak S. Comparison of the thermal reactivities of isolated lignin and holocellulose during pyrolysis. Fuel Process Technol 2010;91:759–64.
[7] Shafizadeh F. Introduction to the pyrolysis of biomass. J Anal Appl Pyrol 1982;3:283–305.
[8] Yu J, Paterson N, Blamey J, Millan M. Cellulose, xylan and lignin interactions during pyrolysis of lignocellulosic biomass. Fuel 2017;191:140–9.
[9] Yang H, Yan R, Chen H, Lee DH, Zheng C. Characteristics of hemicellulose, cellulose and lignin pyrolysis. Fuel 2007;86:1781–8.
[10] Zabaniotou AA. Pyrolysis of forestry biomass by-products in greece. Energy Sour 1999;21:395–403.
[11] Sharma A, Pareek V, Zhang DK. Biomass pyrolysis-a review of modelling, process parameters and catalytic studies. Renew Sustain Energy Rev 2015;50:1081–96.
[12] Jolly WM, Butler B. Linking photosynthesis and combustion characteristics in live fuels: the role of soluble carbohydrates in fuel preheating. Final Report for JFSP Project ID: 10-1-08-6, Joint Fire Science Program; 2015.
[13] Jolly WM, Hadlow AM, Huguet K. De-coupling seasonal changes in water content and dry matter to predict live conifer foliar moisture content. Int J Wildland Fire 2014;23:480–9.
[14] Jolly WM, Johnson DM. Pyro-ecophysiology: Shifting the paradigm of live wildland fuel research. Fire 2018;1:8.
[15] Countryman CM. Physical characteristics of some northern California brush fuels. USDA Forest Service Report PSW-61; 1982.
[16] Ningbo G, Baoling L, Aimin L, Juanjuan L. Continuous pyrolysis of pine sawdust at different pyrolysis temperatures and solid residence times. J Anal Appl Pyrol 2015;114:155–62.
[17] Ceylan S, Topcu Y. Pyrolysis kinetics of hazelnut husk using thermogravimetric analysis. Bioresour Technol 2014;156:182–8.
[18] Chen Z, Zhu Q, Wang X, Xiao B, Liu S. Pyrolysis behaviors and kinetic studies on eucalyptus residues using thermogravimetric analysis. Energy Convers Manage 2015;105:251–9.
[19] Ozsin G, Putun AE. Kinetics and evolved gas analysis for pyrolysis of food processing wastes using tga/ms/ft-ir. Waste Manage 2017;64:315–26.
[20] Ansah E, Wang L, Shahbazi A. Thermogravimetric and calorimetric characteristics during co-pyrolysis of municipal solid waste components. Waste Manage 2016;56:196–206.
[21] DiBlasi C. Numerical simulation of cellulose pyrolysis. Biomass Bioenergy 1994;7:87–98.
[22] Lewis AD, Fletcher TH. Prediction of sawdust pyrolysis yields from a flat-flame burner using the CPD model. Energy Fuels 2013;27:942–53.
[23] Vizzini G, Bardi EBA, Calcitelli M, Tognotti L. Prediction of rapid biomass devolatilization yields with an upgraded version of the bio-CPD model. In: 31st Meeting of the Italian Section of the Combustion Institute. Torino, Italy; 2008.
[24] Imam T, Capareda S. Characterization of bio-oil, syn-gas and bio-char from switchgrass pyrolysis at various temperatures. J Anal Appl Pyrol 2012;93:170–7.
[25] Isahak WNRW, Hisham MWM, Yarmo MA, Yun Hin T-Y. A review on bio-oil production from biomass by using pyrolysis method. Renew Sustain Energy Rev 2012;16:5910–23.
[26] Bridgwater AV. Review of fast pyrolysis of biomass and product upgrading. Biomass Bioenergy 2012;38:68–94.
[27] Lazzari E, Schena T, Primaz CT, da Silva Maciel GP, Machado ME, Cardoso CAL, et al. Production and chromatographic characterization of bio-oil from the pyrolysis of mango seed waste. Ind Crops Prod 2016;83:529–36.
[28] Effendi A, Gerhauser H, Bridgwater AV. Production of renewable phenolic resins by thermochemical conversion of biomass: a review. Renew Sustain Energy Rev 2008;12:2092–116.
[29] Jahirul M, Rasul M, Chowdhury A, Ashwath N. Biofuels production through biomass pyrolysis—a technological review. Energies 2012;5:4952–5001.
[30] Luo G, Chandler DS, Anjos LCA, Eng RJ, Jia P, Resende FLP. Pyrolysis of whole wood chips and rods in a novel ablative reactor. Fuel 2017;194:229–38.
[31] McKendry P. Energy production from biomass (part 2): conversion technologies. Bioresour Technol 2002;83:47–54.
[32] Papari S, Hawboldt K. A review on the pyrolysis of woody biomass to bio-oil: focus on kinetic models. Renew Sustain Energy Rev 2015;52:1580–95.
[33] Horne PA, Williams PT. Influence of temperature on the products from the flash pyrolysis of biomass. Fuel 1996;75:1051–9.
[34] Onay O, Kockar OM. Slow, fast and flash pyrolysis of rapeseed. Renew Energy 2003;28:2417–33.
[35] Bridgwater AV, Meier D, Radlein D. An overview of fast pyrolysis of biomass. Org Geochem 1999;30:1479–93.
[36] Weise DR, Wright CS. Wildland fire emissions, carbon and climate: characterizing wildland fuels. For Ecol Manage 2014;317:26–40.
[37] Prince DR, Fletcher TH. Differences in burning behavior of live and dead leaves, part 1: measurements. Combust Sci Technol 2014;186:1844–57.
[38] McAllister S, Grenfell I, Hadlow A, Jolly WM, Finney M, Cohen J. Piloted ignition of live forest fuels. Fire Saf J 2012;51:133–42.
[39] Byram GM. Forest fire behavior. In: Davis KP, editor. Forest fire: control and use. New York: McGraw-Hill; 1959. p. 90–123.
[40] Bradbury AW, Sakai Y, Shafizadeh F. A kinetic model for pyrolysis of cellulose. J Appl Polym Sci 1979;23:3271–80.
[41] Diebold JP. A unified, global-model for the pyrolysis of cellulose. Biomass Bioenergy 1994;7:75–85.
[42] Rao TR, Sharma A. Pyrolysis rates of biomass materials. Energy 1998;23:973–8.
[43] Babu BV. Biomass pyrolysis: a state-of-the-art review. Biofuels Bioprod Biorefin 2008;2:393–414.
[44] Safdari M-S, Rahmati M, Amini E, Howarth JE, Berryhill JP, Dietenberger M, et al. Characterization of pyrolysis products from fast pyrolysis of live and dead vegetation native to the southern United States. Fuel 2018;229:151–66.
[45] Lamorlette A, El Houssami M, Morvan D. An improved non-equilibrium model for the ignition of living fuel. Int J Wildland Fire 2018;27:29.
[46] Viney NR. A review of fine fuel moisture modelling. Int J Wildland Fire 1991;1:215–35.
[47] Hillier JL, Fletcher TH, Solum MS, Pugmire RJ. Characterization of macromolecular structure of pyrolysis products from a Colorado Green River oil shale. Ind Eng Chem Res 2013;52:15522–32.
[48] Safdari M-S, Kariminia H-R, Ghobadi Nejad Z, Fletcher TH. Study potential of indigenous pseudomonas aeruginosa and bacillus subtilis in bioremediation of diesel-contaminated water. Water Air Soil Pollut 2016:228.
[49] Fazlollahi F, Saeidi S, Safdari MS, Sarkari M, Klemes JJ, Baxter LL. Effect of operating conditions on cryogenic carbon dioxide removal. Energy Technol 2017;5:1588–98.
[50] Safdari MS, Kariminia HR, Rahmati M, Fazlollahi F, Polasko A, Mahendra S, et al. Development of bioreactors for comparative study of natural attenuation, biostimulation, and bioaugmentation of petroleum-hydrocarbon contaminated soil. J Hazard Mater 2018;342:270–8.
[51] Babaei A, Mehrnia MR, Shayegan J, Sarrafzadeh M-H, Amini E. Evaluation of nutrient removal and biomass production through mixotrophic, heterotrophic, and photoautotrophic cultivation of chlorella in nitrate and ammonium wastewater. Int J Environ Res 2018;12:167–78.
[52] Akhtar J, Saidina Amin N. A review on operating parameters for optimum liquid oil yield in biomass pyrolysis. Renew Sustain Energy Rev 2012;16:5101–9.
[53] Kar Y. Co-pyrolysis of walnut shell and tar sand in a fixed-bed reactor. Bioresour Technol 2011;102:9800–5.
[54] Morali U, Yavuzel N, Sensoz S. Pyrolysis of hornbeam (carpinus betulus l.) sawdust: Characterization of bio-oil and bio-char. Bioresour Technol 2016;221:682–5.
[55] Pütün AE, Özbay N, Önal EP, Pütün E. Fixed-bed pyrolysis of cotton stalk for liquid and solid products. Fuel Process Technol 2005;86:1207–19.
[56] Krishna BB, Biswas B, Ohri P, Kumar J, Singh R, Bhaskar T. Pyrolysis of cedrus deodara saw mill shavings in hydrogen and nitrogen atmosphere for the production of bio-oil. Renew Energy 2016;98:238–44.
[57] Chen D, Liu D, Zhang H, Chen Y, Li Q. Bamboo pyrolysis using tg–ftir and a lab-scale reactor: analysis of pyrolysis behavior, product properties, and carbon and energy yields. Fuel 2015;148:79–86.
[58] Demiral İ, Eryazıcı A, Şensöz S. Bio-oil production from pyrolysis of corncob (Zea mays l.). Biomass Bioenergy 2012;36:43–9.
[59] Hu Z, Zheng Y, Yan F, Xiao B, Liu S. Bio-oil production through pyrolysis of blue-green algae blooms (bgab): product distribution and bio-oil characterization. Energy 2013;52:119–25.
[60] Aysu T, Küçük MM. Biomass pyrolysis in a fixed-bed reactor: effects of pyrolysis parameters on product yields and characterization of products. Energy 2014;64:1002–25.
[61] Varma AK, Mondal P. Pyrolysis of pine needles: effects of process parameters on products yield and analysis of products. J Therm Anal Calorim 2017.
[62] Özbay N, Apaydın-Varol E, Burcu Uzun B, Eren Pütün A. Characterization of bio-oil obtained from fruit pulp pyrolysis. Energy 2008;33:1233–40.
[63] Majhi A, Sharma YK, Naik DV, Chauhan R. The production and evaluation of bio-oil obtained from the jatropha curcas cake. Energy Sour Part A 2015;37:1782–9.
[64] Uzun BB, Apaydin-Varol E, Ateş F, Özbay N, Pütün AE. Synthetic fuel production from tea waste: characterisation of bio-oil and bio-char. Fuel 2010;89:176–84.
[65] Shadangi KP, Mohanty K. Thermal and catalytic pyrolysis of karanja seed to produce liquid fuel. Fuel 2014;115:434–42.
[66] Bordoloi N, Narzari R, Sut D, Saikia R, Chutia RS, Kataki R. Characterization of bio-oil and its sub-fractions from pyrolysis of scenedesmus dimorphus. Renew Energy 2016;98:245–53.
[67] Abnisa F, Daud WMAW, Husin WNW, Sahu JN. Utilization possibilities of palm shell

as a source of biomass energy in Malaysia by producing bio-oil in pyrolysis process. Biomass Bioenergy 2011;35:1863–72.
[68] Fu P, Yi W, Bai X, Li Z, Hu S, Xiang J. Effect of temperature on gas composition and char structural features of pyrolyzed agricultural residues. Bioresour Technol 2011;102:8211–9.
[69] Uçar S, Karagöz S. The slow pyrolysis of pomegranate seeds: The effect of temperature on the product yields and bio-oil properties. J Anal Appl Pyrol 2009;84:151–6.
[70] Encinar JM, Gonzalez JF, Gonzalez J. Fixed-bed pyrolysis of cynara cardunculus l. Product yields and compositions. Fuel Process Technol 2000;68:209–22.
[71] Chen D, Li Y, Cen K, Luo M, Li H, Lu B. Pyrolysis polygeneration of poplar wood: effect of heating rate and pyrolysis temperature. Bioresour Technol 2016;218:780–8.
[72] Chen D, Zhou J, Zhang Q. Effects of heating rate on slow pyrolysis behavior, kinetic parameters and products properties of moso bamboo. Bioresour Technol 2014;169:313–9.
[73] Farag S, Fu D, Jessop PG, Chaouki J. Detailed compositional analysis and structural investigation of a bio-oil from microwave pyrolysis of kraft lignin. J Anal Appl Pyrol 2014;109:249–57.